CHEMISTRY OF MATERIALS

Article

pubs.acs.org/cm

# Highly Selective Chemical Vapor Deposition of Tin Diselenide Thin Films onto Patterned Substrates via Single Source Diselenoether Precursors

C. H. (Kees) de Groot,[†] Chitra Gurnani,[‡] Andrew L. Hector,[‡] Ruomeng Huang,[†] Marek Jura,[§] William Levason,[‡] and Gillian Reid*[,‡]

[†]School of Electronics and Computer Science and [‡]School of Chemistry, University of Southampton, Southampton SO17 1BJ, U.K.
[§]ISIS, STFC, Harwell Innovation Campus, Didcot, Oxfordshire, OX11 0QX, U.K.

Supporting Information

**ABSTRACT:** The distorted octahedral complexes $[SnCl_4\{^nBuSe(CH_2)_nSe^nBu\}]$ ($n$ = 2 or 3), (**1**) and (**2**), obtained from reaction of $SnCl_4$ with the neutral bidentate ligands and characterized by IR/Raman and multinuclear ($^1H$, $^{77}Se\{^1H\}$ and $^{119}Sn$) NMR spectroscopy and X-ray crystallography, serve as very effective single source precursors for low pressure chemical vapor deposition (LPCVD) of microcrystalline, single phase tin diselenide films onto $SiO_2$, Si and TiN substrates. Scanning Electron Microscopy (SEM) and Atomic Force Microscopy (AFM) imaging show hexagonal plate crystallites which grow perpendicular to the substrate surface in the thicker films, but align mostly parallel to the surface when the quantity of reagent is reduced to limit the film thickness. X-ray diffraction (XRD) and Raman spectroscopy on the deposited films are consistent with hexagonal $SnSe_2$ ($P\bar{3}m1$; $a = b = 3.81$ Å; $c = 6.13$ Å), with strong evidence for preferred orientation of the crystallites in thinner (0.5−2 μm) samples, consistent with crystal plate growth parallel to the substrate surface. Hall measurements show the deposited $SnSe_2$ is a n-type semiconductor. The resistivity of the crystalline films is 210 (±10) mΩ cm and carrier density is $5.0 \times 10^{18}$ $cm^{-3}$. Very highly selective film growth from these reagents onto photolithographically patterned substrates is observed, with deposition strongly preferred onto the (conducting) TiN surfaces of $SiO_2$/TiN patterned substrates, and onto the $SiO_2$ surfaces of Si/$SiO_2$ patterned substrates. A correlation between the high selectivity and high contact angle of a water droplet on the substrate surfaces is observed.

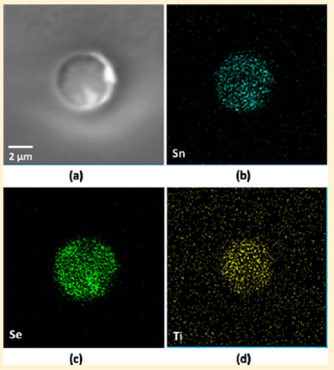


**KEYWORDS:** *tin diselenide, chemical vapor deposition, selective deposition, single source precursor, selenoether complexes*

## 1. INTRODUCTION

Metal chalcogenides form an extremely important class of layered semiconductor materials that find a range of applications in modern electronics. Many of these materials can be deposited via chemical vapor deposition (CVD) techniques, and this has stimulated a large amount of work on the development of tailored CVD precursors for their production.[1] Within the chalcogenide-based materials, the narrow band gap semiconductors $Sb_2E_3$ and $Bi_2E_3$ (E = Se or Te) are important thermoelectric materials,[2] which are also attracting considerable interest as topological insulators,[3] while early transition metal chalcogenides such as $TiE_2$ (E = S, Se, Te) are useful cathode materials in batteries.[4] Binary and ternary chalcogenides are also of considerable interest as solid state phase change memory (PCM) materials for data storage as a result of the different resistivities of the crystalline and amorphous phases. For this application key considerations are the resistivity ratio, energy requirements and cyclability of switching between their amorphous and crystalline states. Most PCM materials are based upon selenide or telluride alloys of main group elements and they are widely regarded as realistic competitors for Flash memory in the consumer electronics markets.[5] $Ge_2Sb_2Te_5$ (GST-225) has excellent characteristics for this purpose and is currently the preferred material in industry, although the production and phase change properties of a wide range of different PCM materials are being investigated to optimize the rates of switching between the amorphous and crystalline phases, and to seek materials where the differences in resistivity between the phases is maximized. Tin selenide is a narrow band gap (ca. 0.9 eV) semiconductor and is of interest for a number of optical and electronic applications.[6−8] Recently $SnSe_2$ has attracted significant interest as a PCM material because of its very fast recrystallization times (~20 ns), which are comparable to those of GST-225 and its high resistivity contrast ($10^5$).[9,10] These films were produced either via spin-coating (using $[hydrazinium]_4[Sn_2Se_6]$,[11] followed by thermal decomposition (573 K),[9] or via molecular beam epitaxy.[10]

Organoselenium compounds such as metal selenolates have been shown to be useful reagents for single source CVD of metal selenide thin films,[12,13] and tend to be based upon

**Received:** September 5, 2012
**Published:** October 18, 2012





dx.doi.org/10.1021/cm302864x | *Chem. Mater.* 2012, 24, 4442−4449

monodentate selenolate ligands because of the practical challenges in forming chelating selenolates and their extreme moisture and oxygen sensitivities. O'Brien and co-workers have developed single source precursors for CVD of metal selenide films and nanoparticles based upon a wide range of molecular dialkyldiselenocarbamato complexes.[1] Neutral thio- and selenoether ligands ($SR_2$, $SeR_2$) form complexes with a very wide range of d- and p-block acceptors,[14] and can coordinate to a variety of metal oxidation states, including even very high oxidation states such as Ta(V), Nb(V), V(IV), and Ti(IV),[15] as well as Sn(IV).[16] Further, a range of ligand architectures (variations in interdonor linkages) and denticities may be accessed readily,[17] in principle permitting fine-tuning of the ligand and complex properties. An important consideration in chalcogenoether chemistry is the trends in E−C bond strengths, which decrease significantly with heavier E (due mainly to the orbital energy mismatch between C and E).[18] Few CVD precursors based on neutral thioether or selenoether compounds have been reported. Notable examples include dual source atmospheric pressure CVD of metal selenides using $SeEt_2$ with volatile metal chlorides or amides,[19] although small differences in deposition conditions can lead to mixed phases, and a large excess of $SeEt_2$ is necessary to form pure $SnSe_2$. A small number of selenoether complexes $[TiCl_4(SeEt_2)_2]$[20] and $[TiCl_4\{o\text{-}C_6H_4(CH_2SeMe)_2\}]$[21] have been used as single source precursors for low pressure CVD of $TiSe_2$. While single source precursors ought, in principle, to be more efficient CVD reagents, offering greater control of metal:chalcogen and improved reagent efficiency, in practice this is not always the case. For example, $[SnCl_4(SeEt_2)_2]$ and $[SnCl_4\{o\text{-}C_6H_4(CH_2EMe)_2\}]$ have been shown to deposit both tin monochalcogenide and tin dichalcogenide by low pressure (LP) CVD depending upon the conditions.[21]

CVD is a widely used deposition process in industry for semiconductor alloys, with most processes using dual or multiple sources, often based on metal alkyls, amides or alkoxides. However, one well-known limitation of CVD is that it usually offers little spatial control over where the deposition occurs (leading to poor precursor efficiency) and also that filling small features is often difficult. While substrate selective CVD of semiconductors is known and can lead to deposition of different film morphologies,[22] examples of area selective binary (or ternary) compound semiconductor deposition via CVD are rare, and to our knowledge there are none based upon single source CVD reagents. Notable examples via dual/multiple source CVD are the selective growth of InAs self-assembled quantum dots on nanopatterned $SiO_2$/Si substrate (from $Me_3In$ and $Me_3As$)[23] and $Ge_2Sb_2Te_5$.[24] Atomic layer deposition (ALD) of conformal coatings of $(GeTe_2)_{(1-x)}(Sb_2Te_3)_x$ within 120 nm diameter pores has been demonstrated very recently using $Te(SiMe_3)_2$, $Ge(OMe)_4$, and $Sb(OEt)_3$.[25]

We report here the low pressure chemical vapor deposition (LPCVD) of single phase, crystalline $SnSe_2$ thin films onto a range of substrates (Si, $SiO_2$, and TiN) using the molecular single source precursors $[SnCl_4\{^nBuSe(CH_2)_nSe^nBu\}]$ ($n$ = 2 or 3), that is, tin(IV) chloride complexes with neutral chelating selenoether ligands. Compositional (energy dispersive X-ray (EDX) and X-ray photoelectron spectroscopy (XPS)), structural (Raman, X-ray diffraction (XRD), scanning electron microscopy (SEM), and atomic force microscopy (AFM)), and electrical (Hall measurements) data are presented, as well as demonstration of control of the film thickness and crystallite orientation by varying the quantity of precursor and deposition time. Very unusually, the new reagents also allow *highly selective* deposition of $SnSe_2$ thin films into small TiN "holes" (5 $\mu$m diameter, 1 $\mu$m deep) within photolithographically patterned substrates (TiN/$SiO_2$); the possible origins of this exceptional selectivity are discussed.

## 2. EXPERIMENTAL SECTION

**2.1. Precursor Preparation and Characterization.** All reactions were conducted using Schlenk, vacuum line and glovebox techniques under a dry nitrogen atmosphere. The reagents were stored and manipulated using a glovebox. Hexane, toluene, diethyl ether, and tetrahydrofuran (thf) were dried by distillation over sodium/benzophenone. Dichloromethane was dried over $CaH_2$. $SnCl_4$ and $^n$BuLi (1.6 mol dm$^{-3}$ in diethyl ether) were obtained from Aldrich and used as received. IR spectra were recorded as Nujol mulls between CsI plates using a Perkin-Elmer Spectrum 100 instrument. Raman spectra on the molecular complexes were obtained using a Perkin-Elmer FT2000R with a Nd:YAG laser. $^1$H NMR spectra were recorded from solutions in $CD_2Cl_2$ on a Bruker AV300, $^{77}$Se{$^1$H} and $^{119}$Sn NMR spectra on a Bruker DPX400 and referenced to external neat $SeMe_2$ and $SnMe_4$ respectively. Microanalytical results were from Medac Ltd.

*$^nBuSe(CH_2)_3Se^nBu$.* Freshly ground selenium powder (5.0 g, 0.063 mol) in dry thf (140 mL) was frozen in a liquid nitrogen bath. $^n$BuLi (40 mL of 1.6 mol dm$^{-3}$ solution in diethyl ether, 0.063 mol) was added and the mixture allowed to thaw, and then stirred at room temperature for 2 h to give a colorless solution. 1,3-Dichloropropane (3 mL, 3.57 g, 0.03 mol) was added dropwise to the mixture which was then refluxed 1 h. Hydrolysis (aqueous saturated NaCl, 100 mL) was followed by separation, extraction with diethyl ether, and drying ($MgSO_4$). The solvent was removed by distillation, and the residue fractionated in vacuo to give pale yellow oil. Yield: 5.0 g, 50%. $^1$H NMR ($CDCl_3$) $\delta$/ppm: 0.90 (t, [6H], $CH_3$), 1.39 (m, [4H], $CH_2$), 1.62 (m, [4H], $CH_2$), 1.97 (m, [2H], $CH_2$), 2.54 (m, [4H], $CH_2Se$), 2.62 (s, [4H], $SeCH_2$). $^{13}$C{$^1$H} NMR ($CDCl_3$) $\delta$/ppm: 13.59 ($CH_3$), 23.02 ($CH_2$), 23.56 ($CH_2Se$, $^1J_{SeC}$ = 60 Hz), 23.75 ($CH_2Se$, $^1J_{SeC}$ = 60 Hz), 31.26 ($CH_2$), 32.71 ($CH_2$). $^{77}$Se{$^1$H} NMR (neat) $\delta$/ppm: 156.

*$^nBuSe(CH_2)_2Se^nBu$.* Prepared as above, but using 1,2-dichloroethane. Yield: 5.0 g, 50%. $^1$H NMR ($CDCl_3$) $\delta$/ppm: 0.92 (t, [6H], $CH_3$), 1.42 (m, [4H], $CH_2$), 1.66 (m, [4H], $CH_2$), 2.62 (m, [4H], $CH_2Se$), 2.84(s, [4H], $SeCH_2$). $^{13}$C{$^1$H} NMR ($CDCl_3$) $\delta$/ppm: 13.59 ($CH_3$), 23.02 ($CH_2$), 23.80 ($CH_2Se$, $^1J_{SeC}$ = 60 Hz), 23.93 ($CH_2Se$, $^1J_{SeC}$ = 61 Hz), 32.78 ($CH_2$). $^{77}$Se{$^1$H} NMR (neat) $\delta$/ppm: 205.

*$[SnCl_4\{^nBuSe(CH_2)_2Se^nBu\}]$, (1).* $SnCl_4$ (0.260 g, 1.00 mmol) was added to solution of $^nBuSe(CH_2)_2SeBu^n$ (0.300 g, 1.00 mmol) in anhydrous $CH_2Cl_2$ (10 mL) at room temperature with constant stirring. A pale yellow solution was obtained immediately. After stirring for 30 min, the solution was concentrated in vacuo yielding an off-white precipitate which was collected by filtration, washed with hexane and dried in vacuo. Crystals were obtained by cooling the $CH_2Cl_2$ filtrate from the reaction synthesis at about −18 °C. Yield: 0.35 g, 62%. Anal. Calcd for $C_{10}H_{12}Cl_4Se_2Sn{\cdot}0.5CH_2Cl_2$: C 20.9, H 3.6. Found: C 20.7, H 3.8%. $^1$H NMR ($CDCl_3$, 298 K) $\delta$/ppm: 0.91 (t, [6H], $CH_3$), 1.42 (m, [4H], $CH_2$), 1.78 (m, [4H], $CH_2$), 3.03 (s, [4H], $SeCH_2$), 3.28 (m, [4H], $SeCH_2CH_2Se$), 5.30 ($CH_2Cl_2$); (193 K) $\delta$/ppm: 0.91 (t, [6H], $CH_3$), 1.42 (m, [4H], $CH_2$), 1.76 (m, [4H], $CH_2$), 3.15 (m, [4H], $SeCH_2$), 3.60 (m, [4H], $SeCH_2CH_2Se$), 5.34 ($CH_2Cl_2$). $^{119}$Sn NMR ($CH_2Cl_2$/$CDCl_3$, 298 K): no resonance observed; (193 K) $\delta$/ppm: −626, −649 (ratio ~3:1). $^{77}$Se{$^1$H} NMR ($CH_2Cl_2$, 298 K): no resonance observed; (193 K) $\delta$/ppm: 201, 231 (ratio ~3:1). IR (Nujol) $\nu$/cm$^{-1}$: 264 (w), 309 (s), 320 (s) Sn−Cl. Raman $\nu$/cm$^{-1}$: 236 (s), 264 (s), 319 (s) Sn−Cl.

*$[SnCl_4\{^nBuSe(CH_2)_3Se^nBu\}]$, (2).* $SnCl_4$ (0.130 g, 0.5 mmol) was added to a solution of $^nBuSe(CH_2)_3SeBu^n$ (0.157 g, 0.5 mmol) in anhydrous $CH_2Cl_2$ (10 mL) at room temperature with constant stirring. A yellow solution was obtained immediately. After stirring for 30 min, the solution was concentrated in vacuo yielding a pale yellow precipitate which was collected by filtration, washed with hexane and dried in vacuo. Yield: 0.19 g, 65%. Calc. For $C_{11}H_{24}Cl_4Se_2Sn$: C 22.9, H 4.2. Found: C 23.6, H 4.5%. $^1$H NMR ($CDCl_3$, 298 K) $\delta$/ppm: 0.98


dx.doi.org/10.1021/cm302864x | *Chem. Mater.* 2012, 24, 4442−4449

(t, [6H], $CH_3$), 1.48 (m, [4H], $CH_2$), 1.83 (m, [4H], $CH_2$), 2.53 (m, [2H], $CH_2$), 3.30 (m, [4H], $CH_2Se$), 3.41 (m, [4H], $SeCH_2$). $^{119}$Sn NMR ($CH_2Cl_2$/$CDCl_3$, 298 K): no resonance observed; (190 K) $\delta$/ppm: −695 ($^1J_{SnSe}$ = 505 Hz). $^{77}$Se{$^1$H} NMR ($CD_2Cl_2$, 185 K) $\delta$/ppm: 290. IR (Nujol) $\nu$/cm$^{-1}$: 311 (br) Sn−Cl. Raman $\nu$/cm$^{-1}$: 270 (s), 319 (s) Sn−Cl. Thermogravimetric analysis (performed in a dry, $N_2$ purged glovebox) shows complete sublimation, with $T_{sub}$ = 563 K.

*X-ray Crystallography.* Crystals of (**1**) suitable for single-crystal X-ray analysis were obtained by cooling the filtrate ($CH_2Cl_2$) from the complex preparation. Data collection used a Bruker-Nonius Kappa CCD diffractometer fitted with monochromated Mo−$K_\alpha$ radiation ($\lambda$ = 0.71073 Å), with the crystals held at 120 K in a nitrogen gas stream. Structure solution and refinement were straightforward,[26,27] with H atoms introduced into the model in idealized positions. Crystal structure of [$SnCl_4${$^n$BuSe$(CH_2)_2$Se$^n$Bu}], (**1**): formula = $C_{10}H_{22}Cl_4Se_2Sn$, $M$ = 560.69, crystal system monoclinic, space group $C2/c$ (no. 15), $a$ = 9.186(2), $b$ = 11.811(4), $c$ = 17.1785(10) Å, $\beta$ = 102.432(4)°, Vol = 1820.0(7) Å$^3$, $\mu$ = 5.972 mm$^{-1}$, total no. of reflections measured =7590, $R_{int}$ = 0.0455, 2079 unique reflections, 79 independent parameters, R1 ($I > 2\sigma I$) = 0.034, R1 (all data) = 0.040, wR2 ($I > 2\sigma I$) = 0.075, wR2 (all data) = 0.079.

**2.2. $SnSe_2$ Film Characterization.** XRD patterns were collected in grazing incidence ($\theta_1$ = 3°) using a Bruker D8 with GADDS diffractometer (Cu−$K_{\alpha 1}$) except to look for preferred orientation, when a Siemens D5000 Bragg−Brentano system (Cu−$K_{\alpha 1}$) was used. Preferred orientation was modeled by generating a dummy histogram using the GSAS package[28] from a standard literature $SnSe_2$ pattern.[29] The March-Dollase preferred orientation ratio was manually varied until the intensities of the diffraction reflections closely resembled those in the observed patterns. The texture coefficient was obtained by dividing the average change in intensity for reflections associated with the relevant crystallographic direction by an average of the intensity change across all reflections.[30] Raman scattering spectra of the deposited films were measured at room temperature on a Renishaw InVia Micro Raman Spectrometer using a helium−neon laser with a wavelength of 632.8 nm. The incident laser power was adjusted to ∼1 mW for all samples. X-ray photoelectron spectroscopy (XPS) data were obtained using a Thermo Scientific Theta Probe System with Al−$K_\alpha$ radiation (photon energy = 1486.6 eV). Where necessary, sample charging was eliminated by use of an electron flood gun delivering 5 eV electrons. The Sn 3d, Se 3d, and C 1s spectra were collected. The Thermo Advantage software was used for data analysis. Data were referenced to the C 1s peak, which was assigned a binding energy of 284.8 eV. Scanning electron microscopy (SEM) was performed on samples at an accelerating voltage of 10 kV using a Zeiss EVO LS 25, and energy dispersive X-ray (EDX) data were obtained with an Oxford INCAx-act X-ray detector. The cross-section SEM measurements were carried out with a field emission SEM (Jeol JSM 7500F) at an accelerating voltage of 2 kV. Atomic force microscopy (AFM) was conducted using a Veeco Dimension 3100 in tapping mode. Hall measurements were performed at room temperature on a Nanometrics HL5500PC with a current of 1 mA. Contact angles were determined using a Krauss DSA100 Drop shape Analyzer purpose built arrangement assembled on a vibrationally isolated platform. The drop of water was expelled through a microsyringe onto the surface of the substrate. The contact angle ($\theta$) was measured using a microscope equipped with a goniometer. The contact angle was estimated as the tangent normal to the drop at the intersection between the sessile drop and the surface. All reported contact angles are the average of at least three measurements taken at different locations and have a maximum error of ±2°.

**2.3. Substrate Preparation and Pretreatment.** TiN films with thickness of 100 nm were deposited on a p-type Si (100) wafer by the medium frequency magnetron sputtering method (Leybold HELIOS Pro) at room temperature. The films were deposited from a Ti (99.99% purity) target with a direct current (DC) power of 3000 W in a $N_2$/Ar atmosphere. The $N_2$ and Ar flow rates were maintained at 30 and 35 sccm respectively. A high drive speed of 180 rpm was applied to enhance the film uniformity. The deposition rate was found to be 0.161 nm s$^{-1}$. $SiO_2$ films with thickness of 1 $\mu$m were also formed by the medium frequency magnetron sputtering method using a pure Si (99.99% purity) target with a DC power of 2000 W in an $O_2$/Ar atmosphere. The $O_2$ and Ar flow rates were maintained at 20 and 40 sccm respectively. With the same drive speed of 180 rpm, the deposition rate was 0.3 nm s$^{-1}$. The patterned samples were fabricated via a photolithographic process followed by a reactive-ion etching of $SiO_2$. The pattern was predesigned on a mask with template hole-sizes ranging from 1 to 100 $\mu$m. The photolithography was carried out using an EVG 620TB with a positive resist S1813. The etching was performed by a RIE80+ with $CHF_3$ and Ar. The etching rate was found to be 0.37 nm s$^{-1}$.

Prior to LPCVD experiments the silica tile substrates (ca. 1 × 5 × 25 mm) used for the depositions were previously cleaned with acetone and demineralized water and dried at 100 °C overnight. The silicon tiles (1 × 5 × 25 mm) were suspended over 40% HF solution for 15 min, then immediately transferred to a Schlenk tube and heated in vacuo at 110 °C for about 6 h to ensure complete removal of surface bound $H_2O$ (this completely eliminated tin oxide formation during subsequent deposition experiments).

**2.4. LPCVD onto Unpatterned Substrates Using (1) and (2).** In a typical experiment the reagent (20−100 mg) and substrates were loaded into a closed-end silica tube in a glovebox (precursor at the closed end, followed by either Si, $SiO_2$, or TiN substrates positioned end-to-end through the heated region). The tube was set in a furnace such that precursor was outside the heated zone; the tube was evacuated, then heated to 773 K (actual temperature in the hot zone about 767 K) under 0.05 mmHg and the furnace was allowed to stabilize. The tube position was subsequently adjusted so that the precursor was moved toward the hot zone until melting was observed ($T$ ca. 465 K based on temperature profiling carried out after deposition). At this point the sample position was maintained until the solid precursor had melted and completely evaporated (no residual precursor remained), that is, about 1−3 h. No additional Se source was added. The tube was then cooled to room temperature and transferred to the glovebox where the tiles were removed and stored under an $N_2$ atmosphere prior to analysis. The highest degree of substrate coverage was found just outside the furnace hot zone and ∼100 mm from the precursor, where the temperature was about 753−773 K, and these were the films selected for further study. Similar experiments were conducted at 50 degree intervals between 723 and 823 K (all of which gave only $SnSe_2$) and using variable amounts of precursor to control the film thickness.

The LPCVD experiments produced silvery-black, reflective films. Both precursors (**1**) and (**2**) gave $SnSe_2$ films, with no significant differences in appearance or properties observed across the deposition temperatures used. Samples were generally very well adhered to the tiles. Excellent reproducibility was obtained, and films were visually very similar between depositions conducted across the temperature range. Similar characterization data were obtained from several different samples.

**2.5. LPCVD onto Patterned Si/$SiO_2$ Substrates Using (1) and (2).** TiN/$SiO_2$ or Si/$SiO_2$ patterned substrates (1 × 5 × 25 mm), the latter previously pretreated by HF vapor-etching for 3 min and dried in vacuo at 110 °C for about 6 h, were loaded with 5 mg of reagent into a closed-end silica tube in a glovebox as described above, and depositions were performed similarly over 30 min.

## 3. RESULTS AND DISCUSSION

The preparation, spectroscopic and structural properties of a series of Sn(IV) halide complexes with simple (Me- or Ph-substituted) thio-, seleno-, and telluroether ligands were described by us previously. All of these adopt distorted octahedral coordination environments.[16,31] However, no materials deposition studies were performed on these. Initial investigations examined LPCVD of the complexes [$SnCl_4${$MeSe(CH_2)_nSeMe$}] ($n$ = 2, 3).[16] These experiments were unsuccessful, depositing only a thin dull gray (graphitic C) layer on the $SiO_2$ tiles, which contained no Sn or Se (EDX).


dx.doi.org/10.1021/cm302864x | Chem. Mater. 2012, 24, 4442−4449

This is attributed in part at least to the instability of the Me radical that would be a likely intermediate in decomposition of these complexes. Therefore, the ligand structure was modified to introduce *n*-butyl terminal substituents to enable an easier thermal decomposition pathway. The new ligands $^{n}$BuSe-$(CH_2)_n$Se$^{n}$Bu ($n$ = 2, 3) were prepared as described in the Experimental Section. The moisture-sensitive complexes [$SnCl_4${$^{n}$BuSe$(CH_2)_n$Se$^{n}$Bu}], (**1**) and (**2**) were obtained in good yield by direct reaction of $SnCl_4$ with the ligand in anhydrous $CH_2Cl_2$. The solids were stored and manipulated in an $N_2$ purged, dry (<1 ppm $H_2O$) glovebox and were characterized by IR, Raman, variable temperature $^{1}$H, $^{77}$Se-{$^{1}$H}, and $^{119}$Sn NMR spectroscopy and microanalysis as appropriate. The spectroscopic features of the new complexes are in accord with those of related complexes in the literature.[16,21] The NMR spectroscopic measurements are consistent with fast dissociative exchange and pyramidal inversion occurring at room temperature, but in the case of (**1**), these processes are slowed sufficiently at 193 K such that individual resonances for the *meso* and *DL* forms are evident in the $^{77}$Se{$^{1}$H} and $^{119}$Sn NMR spectra in the expected chemical shift ranges.[16,21] At low temperature (193 K) complex (**2**) shows only one resonance in both the $^{77}$Se{$^{1}$H} and the $^{119}$Sn NMR spectra, but the $^{1}J_{SeSn}$ coupling (605 Hz) is clearly evident. Therefore we assume that either the relative ratio of *meso*:*DL* forms is very disparate such that only one is observed or the chemical shifts of the two forms are accidentally coincidental (the latter seems less likely given that the $^{77}$Se and $^{119}$Sn NMR chemical shift ranges are very wide). The crystal structure of (**1**) shows (Figure 1) a discrete mononuclear

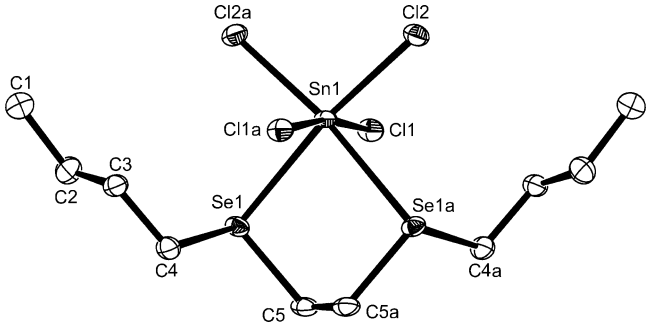


**Figure 1.** View of the crystal structure of (**1**) with atom numbering scheme. H atoms are omitted for clarity, and ellipsoids are drawn at the 50% probability level ellipsoids. The molecule has 2-fold symmetry. Symmetry operation: $a$ = 1 − $x$, $y$, 1/2 − $z$. Selected bond lengths (Å) and angles (deg): Sn1−Cl2 = 2.3829(11), Sn1−Cl1 = 2.4254(11), Sn1−Se1 = 2.7322(7), Cl2−Sn1−Cl2a = 98.04(6), Cl2−Sn1−Cl1 = 93.17(4), Cl2a−Sn1−Cl1 = 93.19(4), Cl1−Sn1−Cl1a = 170.29(5), Cl2−Sn1−Se1 = 171.63(3), Cl2a−Sn1−Se1 = 88.21(3), Cl1−Sn1−Se1 = 80.87(3), Cl1a−Sn1−Se1 = 92.01(3), Se1−Sn1−Se1a = 86.14(3).

molecule with four mutually cis Cl ligands and a chelating diselenoether. The complex has crystallographic 2-fold symmetry (the Sn atom lies on the $C_2$ axis) which places the $^{n}$Bu groups in the *DL* configuration (i.e., the substitutents lie on opposite sides of the $SnSe_2$ plane), and the bond distances and angles around the tin atom are in accord with similar Sn(IV) selenoether species.[16,21]

**3.1. LPCVD Experiments.** Thermogravimetric analysis on (**2**) under a dry $N_2$ atmosphere revealed clean sublimation at 563 K. LPCVD of both selenoether complexes (**1**) and (**2**) was undertaken with the furnace temperature set at a range of temperatures (50 degree intervals) between 673 and 823 K, leading to complete evaporation of the precursor compound and deposition of reflective, silvery-black films onto the $SiO_2$ substrate. Similar behavior was also observed on TiN tiles and clean, dried (after etching with HF vapor) Si tiles. Initially depositions used about 50 to 100 mg of precursor, producing films of thickness about 20 to 60 $\mu$m for compositional and structural characterization. Later depositions were reagent-limited (2−5 mg) to produce films with thicknesses in the range 0.5 to 2 $\mu$m. SEM analysis on the $SnSe_2$ films showed a regular morphology formed of hexagonal plate crystallites (Figure 2a and b) and cross-sectional SEM images of typical

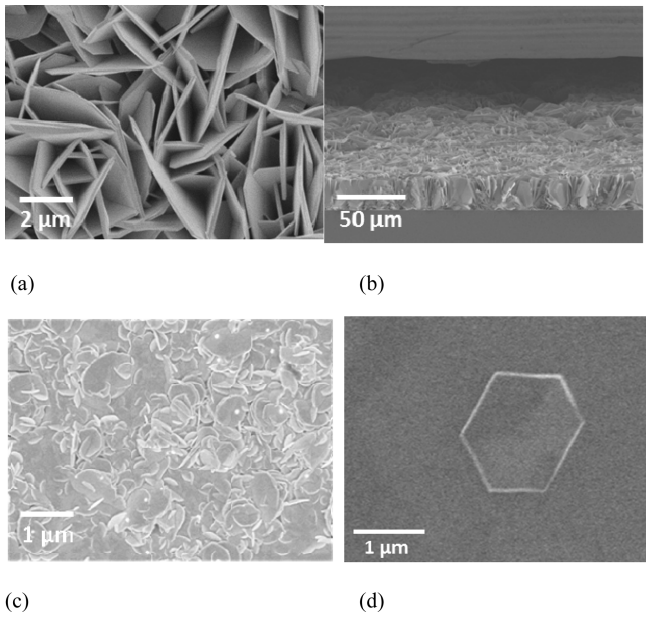


**Figure 2.** SEM images of hexagonal $SnSe_2$: (a) top view and (b) cross section of film deposited from 100 mg of reagent, showing the film thickness of ∼50 $\mu$m both showing the hexagonal crystallites essentially randomly oriented on the substrate; (c) top view of a much thinner (2 $\mu$m) $SnSe_2$ film deposited using 5 mg of reagent (**1**) showing the crystallites mostly lying parallel to the $SiO_2$ substrate; (d) SEM image of a single hexagonal crystallite of about 1.6 $\mu$m across the hexagon.

films grown at between 673 and 823 K using 100 mg of precursor showed these were ∼20 to 60 $\mu$m thick. In these films the growth direction of the crystallites mostly has the *xy* plane close to perpendicular to the surface, but with a significant percentage aligned approximately parallel to the substrate surface. In contrast, reagent-limited films grown using 5 mg of precursor (30 min.) were much thinner as expected (1 to 2 $\mu$m), and SEM image Figure 2c shows the majority of crystallites lying flat on the substrate surface, consistent with the preferred orientation seen by XRD analysis (below); the individual crystallites are about 1.6 $\mu$m × 2.0 $\mu$m across the hexagon (Figure 2d). AFM measurements were consistent with the SEM data, revealing that the thicker $SnSe_2$ film surfaces are considerably rougher than the 0.5−2 $\mu$m samples. RMS roughness measurements on the latter are about 130 nm (2 × 2 $\mu$m scan).

XRD measurements on the materials deposited from (**1**) and (**2**) at various temperatures confirmed them to be crystalline hexagonal $SnSe_2$ in all cases, consistent with space group $P\bar{3}m1$,


dx.doi.org/10.1021/cm302864x | *Chem. Mater.* 2012, 24, 4442−4449

$a$ = 3.81−3.83 Å; $c$ = 6.14−6.16 Å (literature values for bulk $SnSe_2$: $a$ = 3.81 Å; $c$ = 6.14 Å), see Supporting Information,[32] with no evidence for other phases (such as SnSe). There is no significant variation in the lattice parameters of this phase with deposition temperature or with the change in the alkyl linking group in the diselenoether ligand. We saw evidence from the XRD patterns for preferred orientation of the crystallites in the thin (1 to 2 $\mu$m) films where SEM showed crystallites lying flat on the surface (Figure 3), with intense 001 and 002 peaks,

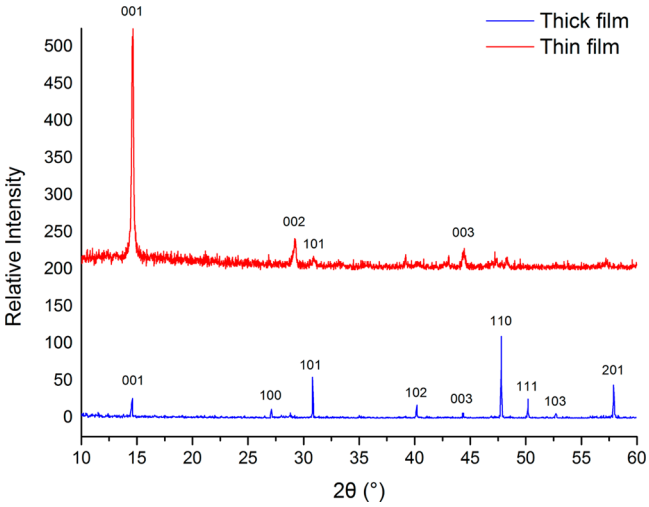


**Figure 3.** XRD of a thick film (bottom) of $SnSe_2$, giving lattice parameters: $a$ = 3.8101(2) Å, $c$ = 6.1347(6) Å; and thin film (top) (the peaks labeled are consistent with $a$ = 3.81 and $c$ = 6.13 Å, although these could not be refined reliably from the small number of diffraction peaks observed. Peaks were indexed using JCPDS file 01-089-3197.

confirming strong alignment of the $c$-axis perpendicular to the substrate surface. The intensities observed were modeled against those from powdered $SnSe_2$ with a level of preferred orientation corresponding to an approximately 3-fold increase in the influence of the $c$-axis. Calculation of a texture coefficient based on the 00l reflections (001, 002, and 003) results in a value for $C_{00l}$ of 2.8. For thick films there is also some preferred orientation observed from the diffraction data. In this case the pattern is closer to the normal powder distribution of intensities, but with enhancement of the 100 and 110 peaks. The texture coefficient based on the $hk0$ reflections (100, 110 and 200), $C_{hk0}$, is 1.6. The level of preferred orientation corresponds to a 2-fold suppression of the peaks related to the $c$-axis.

Previous work using $SeEt_2$ and $SnCl_4$ dual source atmospheric pressure CVD by Carmalt, Parkin, and co-workers,[19] or $[SnCl_4(SeEt_2)_2]$ in single source CVD in our own work,[21] leads to deposition of both $SnSe_2$ and SnSe, with particular care required to restrict the deposition to a single stoichiometry and phase (the dual source approach requiring 10 mol. equiv of $SeEt_2$ to achieve pure $SnSe_2$). However, using the diselenoether precursors described in the present work we have established that single phase $SnSe_2$ only is produced across the temperature range studied, without the need for any added selenoether.

Raman spectra recorded from each thin film sample shows one intense (and sharp) band at 182.4 $cm^{-1}$ (Figure 4), which is assigned to the $A_{1g}$ Raman-active mode of crystalline hexagonal $SnSe_2$,[33] and measurements taken at several locations

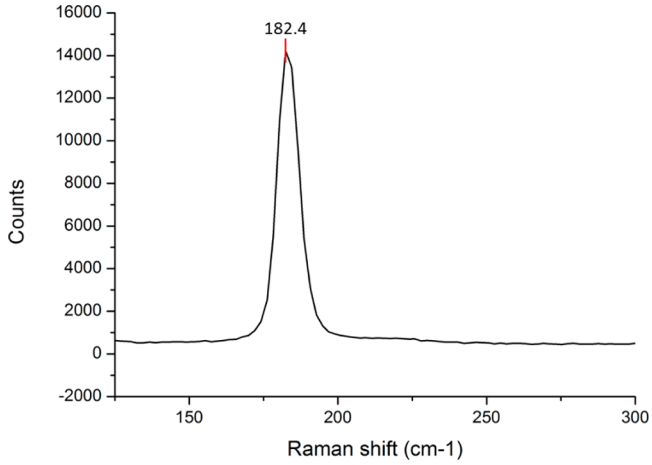


**Figure 4.** Raman spectrum of $SnSe_2$ thin film grown by LPCVD at 773 K from (**1**) showing the $A_{1g}$ mode.

on the sample showed no significant variation in the peak width. .

XPS measurements on unetched ∼40 to 60 $\mu$m samples showed only one Sn and one Se environment (Figure 5), with binding energies corresponding to those reported for $SnSe_2$.[34] For unetched $SnSe_2$ samples C (39.8 wt %) was also evident, but there is no evidence for $SnO_2$, elemental Sn, or elemental Se. Argon ion etching for 60 s resulted in a significant reduction in the carbon content (to 13.0 wt %). The plate crystallite morphology of the $SnSe_2$ samples is likely to lead to inherently higher %C pre-etching because of environmental adsorption of hydrocarbons, and this also precluded complete etching of all of the crystallite surfaces; hence, reliable determination of carbon content from the samples was not possible. The 1:2 Sn:Se ratio was unaffected by etching. EDX measurements on the surface exposed by cross-sectioning the films (i.e., with the incident beam parallel to the substrate) also gave 1:2 Sn:Se ratios. However, as expected the carbon content is considerably lower (2.7%) than that measured by the more surface sensitive XPS.

*Hall Measurements.* For this measurement, $SnSe_2$ was deposited on a $SiO_2$/Si substrate to insulate the current to the substrate. $SnSe_2$ films with thicknesses of 20 and 50 $\mu$m were deposited for the measurement. Both experiments were conducted under a magnetic field of 0.5 T at 300 K. The resistivities for the two $SnSe_2$ films were found to be 210 (±10) mΩ cm. This low level resistivity is consistent with the films being in the crystalline state. The resistivities measured for our samples are about 10 times higher than those reported for other $SnSe_2$ films deposited via spin-coating and annealing or molecular beam epitaxy, 30 mΩ cm[9] and 22 mΩ cm[10] respectively, possibly reflecting the large grain boundary contribution and the different film morphology in the $SnSe_2$ deposits.. The crystalline resistivity of $SnSe_2$ is much higher than that of $Ge_1Sb_2Te_4$ ($\rho$ = 1.6 mΩ cm),[35] which is favorable for PCRAM device applications since a high crystalline resistivity results in a low reset current and hence low power consumption.

The Hall measurements confirmed the $SnSe_2$ deposited by LPCVD in this work to be n type, with mobilities for the two samples of 5.97 $cm^2$/V-s and 2.3 $cm^2$/V-s, respectively, for thicknesses of 50 and 20 $\mu$m. The carrier density was measured as 5.0 × $10^{18}$ $cm^{-3}$, which is in reasonable agreement with $SnSe_2$ films prepared by molecular beam epitaxy.[10]


dx.doi.org/10.1021/cm302864x | *Chem. Mater.* 2012, 24, 4442−4449

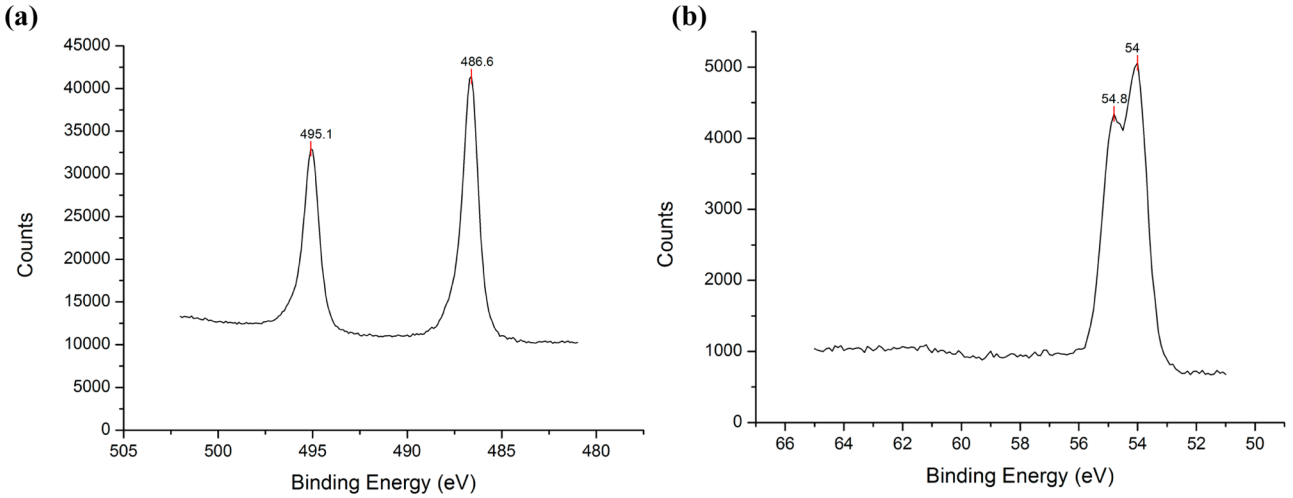


**Figure 5.** XPS data obtained from a representative deposited film of $SnSe_2$ on $SiO_2$ substrate, (a) Sn 3d and (b) Se 3d.

*Selective Deposition.* For many electronic applications it is desirable to be able to deposit the chalcogenide alloy selectively onto specific regions of a patterned substrate, for example, in trenches or holes. Variations in the morphology may also be expected to occur on different substrate types. Hence, deposition experiments were performed under the same conditions onto $SiO_2$, Si, and TiN. While the observed morphology was essentially the same for each substrate type, the SEM data suggested denser film growth onto TiN and $SiO_2$ compared to Si. On this basis a series of reagent-limited LPCVD experiments using 2−5 mg of precursor (deposition time = 30 min.) were undertaken onto photolithographically patterned substrates formed of $SiO_2$/Si. SEM images of the resulting films (Figure 6) show very clearly that $SnSe_2$ film

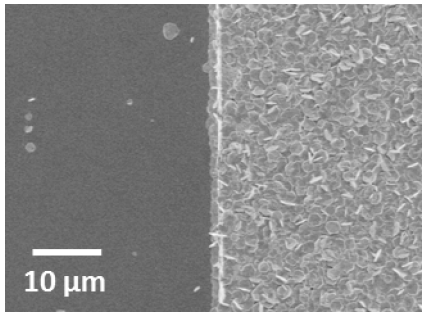


**Figure 6.** SEM image showing selective growth of $SnSe_2$ onto the $SiO_2$ on a patterned Si (left)/$SiO_2$ (right) substrate.

growth onto the $SiO_2$ is preferred, resulting in very high selectivity. For device applications selective deposition onto a conducting surface such as TiN is particularly advantageous. Patterned $SiO_2$/TiN substrates were prepared by growing a layer of $SiO_2$ (1 $\mu$m) onto TiN and photolithograhically etching to form an array of holes with a range of diameters from 1 to 100 $\mu$m (Figure 7). LPCVD of $SnSe_2$ using these structured substrates resulted in remarkably high selectivity for film growth onto the exposed (conducting) TiN regions within the holes, but not onto the $SiO_2$. This was observed both for the large (80−100 $\mu$m diameter) and also for the smaller (5 $\mu$m diameter) holes, as illustrated in Figures 8−10.

This unexpected selectivity of the film growth is also observed for 2 $\mu$m diameter holes, although at this scale the

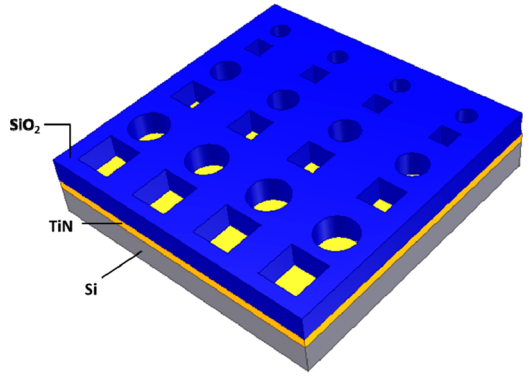


**Figure 7.** Illustration of the photolithographically patterned $SiO_2$/TiN substrates (the $SiO_2$ top layer was grown to 1 $\mu$m thickness).

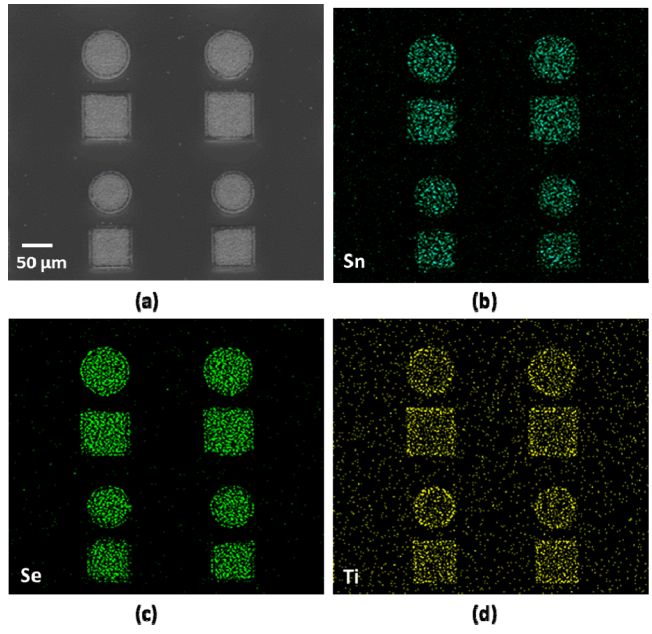


**Figure 8.** SEM image (a) and EDX element maps (b)−(d) confirming the selective deposition of $SnSe_2$ occurring only within the holes (80 $\mu$m diameter) with growth occurring preferentially onto the TiN surface.


dx.doi.org/10.1021/cm302864x | *Chem. Mater.* 2012, 24, 4442−4449

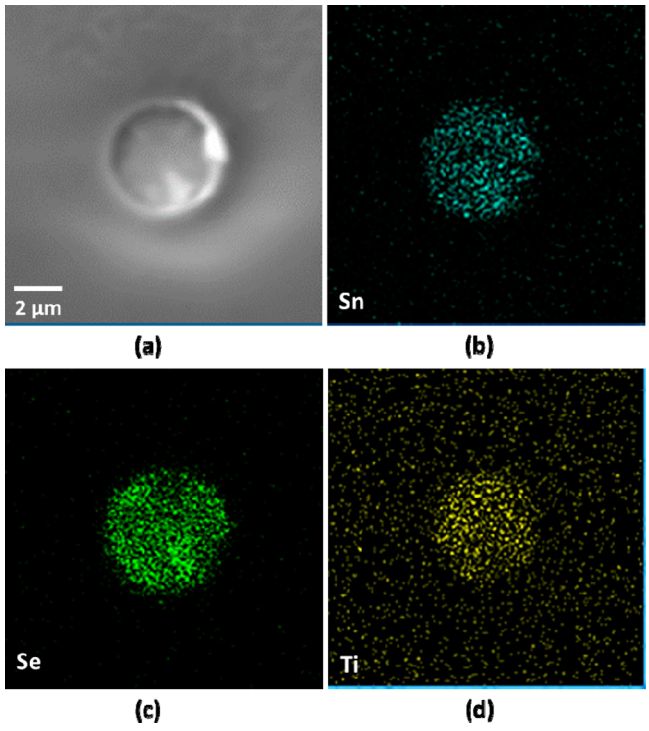


**Figure 9.** SEM image (a) and EDX element maps (b)−(d) confirming the selective deposition of $SnSe_2$ occurring only within the 5 $\mu$m diameter hole, i.e., onto the exposed TiN surfaces.

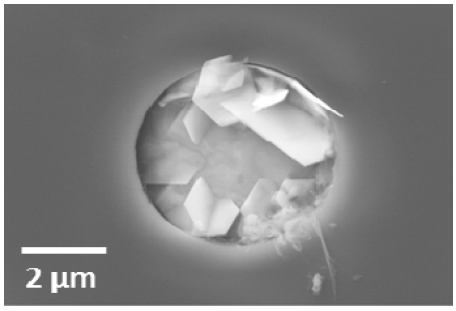


**Figure 10.** SEM image showing the $SnSe_2$ crystallites contained within a 5 $\mu$m diameter hole (TiN) on patterned $TiN/SiO_2$.

selectivity is limited by the size of the individual $SnSe_2$ crystallites (~1.6 × 2.0 $\mu$m across the hexagon), hence while nucleation appears to initiate on the TiN, this then nucleates further crystallite growth onto the $SiO_2$.

AFM measurements confirm that the surface roughness of the different types of substrate are essentially invariant; however, a strong correlation is observed between the contact angle of a water droplet on the surface and the selectivity of the $SnSe_2$ deposition on the substrate surfaces. The measured contact angles increase from Si to $SiO_2$ to TiN ($\theta$/deg: 29, 58, 74, respectively) and selectivity increases across this same series. The selective growth of thin films by CVD is usually governed by the relative rates of nucleation and growth on the different surfaces, although the nucleation stage is generally more important, and so controlling this leads to selectivity, see for example ref 36 and references therein. The contact angle experiments show a strong correlation between higher contact angle (more hydrophobic) surfaces and greater tendency to deposit on that surface. The reason for this may lie in the hydrophobic nature of the *n*-butyl tail groups in the precursor complexes, leading to a higher affinity for adsorption of the precursor onto the most hydrophobic surface (i.e., TiN rather than $SiO_2$ for the $TiN/SiO_2$ patterned substrates and $SiO_2$ rather than Si on the $SiO_2/Si$ patterned substrates). This remarkable selectivity for film deposition from the single source selenoether ligand complexes onto the highly conducting TiN is very attractive for potential applications of chalcogenide materials in electronic devices.

## 4. CONCLUSIONS AND OUTLOOK

The neutral selenoether ligand complexes (**1**) and (**2**) are convenient (scalable) and very effective single source precursors for the growth of single phase, crystalline tin diselenide via LPCVD, without the need for any additional Se source. Preferred crystallite orientation occurs for all the films, but this is different for the thick versus thin films. The SEM and XRD data show that crystallites lie flat (*c*-axis perpendicular to the substrate) in thin films (ca. 0.5−2 $\mu$m), but stand up (*c*-axis close to parallel to the substrate) in thicker (40−60 $\mu$m) films. Hall measurements show the deposited $SnSe_2$ is a n-type semiconductor with the resistivity of the crystalline $SnSe_2$ films an order of magnitude higher than those reported for $SnSe_2$ deposited by spin coating or molecular beam epitaxy (MBE), and with a carrier density comparable to that of reported for $SnSe_2$ formed by MBE, confirming the high quality of the materials formed in this work.

Importantly, the reagents exhibit a very high degree of selectivity onto lithographically patterned substrates, with deposition strongly preferred onto the (conducting) TiN on $SiO_2/TiN$ surfaces, and onto the $SiO_2$ on $Si/SiO_2$ substrates. An empirical correlation is evident between the high selectivity and high contact angle of a water droplet.

The combination of the highly selective growth onto the conducting TiN surfaces within the lithographically formed holes, the preferred *c*-axis alignment observed for these thin films, and the stoichiometric, single phase $SnSe_2$ film deposition are highly relevant to the prospective application of these and related chalocogenoether complexes as single source precursors for chalcogenide materials in electronics, including solid state PCM.

## ■ ASSOCIATED CONTENT

### Supporting Information

Representative XRD pattern for a thick (ca. 40 $\mu$m) $SnSe_2$ film deposited in this work (Figure S1); SEM images showing selective deposition of $SnSe_2$ onto TiN within the 80 $\mu$m diameter holes of a patterned $SiO_2/TiN$ substrate (Figures S2−S4). This material is available free of charge via the Internet at http://pubs.acs.org. CCDC-890352 contains the supplementary crystallographic data for this paper. These data can be obtained free of charge from The Cambridge Crystallographic Data Centre via www.ccdc.cam.ac.uk/data_request/cif.

## ■ AUTHOR INFORMATION

### Corresponding Author

*E-mail: G.Reid@soton.ac.uk.

### Notes

The authors declare no competing financial interest.

## ■ ACKNOWLEDGMENTS

C.G. thanks the Royal Society for a Newton International Fellowship. The authors also thank EPSRC (EP/I010890/1)

for funding, Dr. M. Webster for assistance with the single crystal X-ray diffraction analysis, Dr. S. Pearce for assistance with the TiN and $SiO_2$ sputtering, and STFC for access to AFM facilities in the Materials Characterization Laboratory (MCL) at ISIS.

## REFERENCES

(1) Malik, M. A.; Afzaal, M.; O'Brien, P. *Chem. Rev.* **2010**, *110*, 4417.
(2) For examples see (a) Wang, W.; Poudel, B.; Yang, J.; Wang, D. Z.; Ren, J. F. *J. Am. Chem. Soc.* **2005**, *127*, 13792. (b) Christian, P.; O'Brien, P. *J. Mater. Chem.* **2005**, *15*, 4949.
(3) (a) Xia, Y.; Qian, D.; Hsieh, D.; Wray, L.; Pal, A.; Lin, H.; Bansil, A.; Grauer, D.; Hor, Y. S.; Cava, J.; Hasan, M. Z. *Nat. Phys.* **2009**, *5*, 398.
(4) (a) Gabane, J. P. *Lithium Batteries*; Academic Press: London, U.K., 1983; (b) Whittingham, M. S. *Chem. Rev.* **2004**, *104*, 4271 , and references therein.
(5) Raoux, S.; Wełnic, W.; Ielmini, D. *Chem. Rev.* **2010**, *110*, 240.
(6) Liu, S.; Guo, X.; Li, M.; Zhang, W.-H.; Lui, X.; Li, A. *Angew. Chem., Int. Ed.* **2011**, *50*, 12050.
(7) Bindu, K.; Nair, P. K. *Semicond. Sci. Technol.* **2004**, *19*, 1348.
(8) Achimovičová, M.; da Silva, K. L.; Daneu, N.; Rečnik, A.; Indris, S.; Hain, H.; Scheuermann, M.; Hahn, H.; Šepelák, V. *J. Mater. Chem.* **2011**, *21*, 5873.
(9) Wang, R. Y.; Caldwell, M. A.; Jeyasingh, R. G. D.; Aloni, S.; Shelby, R. M.; Wong, H.-S. P.; Milliron, D. J. *J. Appl. Phys.* **2011**, *109*, 113506.
(10) Chung, K.-M.; Wamwangi, D.; Woda, M.; Wuttig, M.; Bensch, W. *J. Appl. Phys.* **2008**, *103*, 083523.
(11) Mitzi, D. B. *Inorg. Chem.* **2005**, *44*, 3755.
(12) Arnold, J. *Prog. Inorg. Chem.* **1995**, *43*, 353 and references therein.
(13) (a) Hector, A. L.; Levason, W.; Reid, G.; Reid, S. D.; Webster, M. *Chem. Mater.* **2008**, *20*, 5100. (b) Hector, A. L.; Jura, M.; Levason, W.; Reid, S. D.; Reid, G. *New. J. Chem.* **2009**, *33*, 641.
(14) (a) Levason, W.; Reid, G. *J. Chem. Soc., Dalton Trans.* **2001**, 2953. (b) Levason, W.; Reid, G.; Zhang, W. *Dalton Trans.* **2011**, *40*, 8491.
(15) (a) Levason, W.; Patel, B.; Reid, G.; Tolhurst, V.-A.; Webster, M. *J. Chem. Soc., Dalton Trans.* **2000**, 3001. (b) Hart, R.; Levason, W.; Patel, B.; Reid, G. *J. Chem. Soc., Dalton Trans.* **2002**, 3153. (c) Hector, A. L.; Levason, W.; Middleton, A. J.; Reid, G.; Webster, M. *Eur. J. Inorg. Chem.* **2007**, 3655. (d) Jura, M.; Levason, W.; Ratnani, R.; Reid, G.; Webster, M. *Dalton Trans.* **2010**, 883. (e) Benjamin, S. L.; Hyslop, A.; Levason, W.; Reid, G. *J. Fluorine Chem.* **2012**, *137*, 77.
(16) Dann, S. E.; Genge, A. R. J.; Levason, W.; Reid, G. *J. Chem. Soc., Dalton Trans.* **1997**, 2207.
(17) (a) Levason, W.; Reid, G. In *Comprehensive Coordination Chemistry II*; McCleverty, J. A., Meyer, T. J., Eds.; Elsevier: Amsterdam, The Netherlands, 2004; Vol. *1*, p 391. (b) Levason, W.; Reid, G. *Handbook of Chalcogen Chemistry*; Devillanova, F. A., Ed.; Royal Society of Chemistry: Cambridge, U.K., 2007; p 81.
(18) (a) Hope, E. G.; Levason, W. *Coord. Chem. Rev.* **1993**, *122*, 109. (b) Levason, W.; Orchard, S. D.; Reid, G. *Coord. Chem. Rev.* **2002**, *225*, 159.
(19) (a) Boscher, N. D.; Carmalt, C. J.; Palgrave, R. G.; Parkin, I. P. *Thin Solid Films* **2008**, *516*, 4750. (b) Boscher, N. D.; Carmalt, C. J.; Parkin, I. P. *Appl. Surf. Sci.* **2010**, *256*, 3178. (c) Boscher, N. D.; Blackman, C. S.; Carmalt, C. J.; Parkin, I. P.; Garcia Prieto, A. *Appl. Surf. Sci.* **2007**, *253*, 6041. (d) Boscher, N. D.; Carmalt, C. J.; Parkin, I. P. *Eur. J. Inorg. Chem.* **2006**, 1255.
(20) McKarns, P. J.; Lewkebandara, T. S.; Yap, G. P. A.; Liable-Sands, L. M.; Rheingold, A. L.; Winter, C. H. *Inorg. Chem.* **1998**, *37*, 418.
(21) Reid, S. D.; Hector, A. L.; Levason, W.; Reid, G.; Waller, B. J.; Webster, M. *Dalton Trans.* **2007**, 4769.
(22) (a) Edusi, C.; Hyett, G.; Sankar, G.; Parkin, I. P. *Chem. Vap. Deposition* **2011**, *17*, 30. (b) Carmalt, C. J.; Parkin, I. P.; Peters, E. S. *Polyhedron* **2003**, *22*, 1263.
(23) Choi, B. H.; Park, C. M.; Song, S.-H.; Son, M. H.; Hwang, S. W.; Ahn, D.; Kim, E. K. *Appl. Phys. Lett.* **2001**, *78*, 1403.
(24) Choi, B. J.; Choi, S.; Shin, Y. C.; Kim, K. M.; Hwang, C. S.; Kim, Y. J.; Son, Y. J.; Hong, S. K. *Chem. Mater.* **2007**, *19*, 4387.
(25) Eom, T.; Choi, S.; Choi, B. J.; Lee, M. H.; Gwon, T.; Rha, S. H.; Lee, W.; Kim, M.-S.; Xiao, M.; Buchanan, I.; Cho, D.-Y.; Hwang, C. S. *Chem. Mater.* **2012**, *24*, 2099.
(26) Sheldrick, G. M. *SHELXS-97, Program for crystal structure solution*; University of Göttingen: Göttingen, Germany, 1997.
(27) Sheldrick, G. M. *SHELXL-97, Program for crystal structure refinement*; University of Göttingen: Göttingen, Germany, 1997.
(28) (a) Larson, A. C.; von Dreele, R. B. General Structure Analysis System (GSAS). Los Alamos National Laboratory Report LAUR 86-748; Los Alamos National Laboratory: Los Alamos, NM, 2000. (b) Toby, B. H. *J. Appl. Crystallogr.* **2001**, *34*, 210.
(29) Liu, H.; Chang, L. Y. *J. Alloys Compd.* **1992**, *185*, 183.
(30) Karim, S.; Toimil-Molares, M. E.; Maurer, F.; Miehe, G.; Ensinger, W.; Liu, J.; Cornelius, T. W.; Neumann, R. *Appl. Phys. A: Mater. Sci. Process.* **2006**, *84*, 403.
(31) (a) Dann, S. E.; Genge, A. R. J.; Levason, W.; Reid, G. *J. Chem. Soc., Dalton Trans.* **1996**, 4471. (b) Genge, A. R. J.; Levason, W.; Reid, G. *J. Chem. Soc., Dalton Trans.* **1997**, 4549. (c) Davis, M. F.; Levason, W.; Reid, G.; Webster, M.; Zhang, W. *Dalton Trans.* **2008**, 533.
(32) Inorganic Crystal Structure Database (ICSD) Fachinformationszentrum Karlsruhe (FIZ), accessed via the United Kingdom Chemical Database Service: Fletcher, D. A.; McMeeking, R. F.; Parkin, D. *J. Chem. Inf. Comput. Sci.* **1996**, *36*, 746.
(33) (a) Walsh, D.; Jandl, S.; Harbec, J. Y. *J. Phys. C: Solid State Phys.* **1980**, *13*, L125. (b) Smith, A. J.; Meek, P. E.; Liang, W. Y. *J. Phys. C: Solid State Phys.* **1977**, *10*, 1321.
(34) Schlaf, R.; Louder, D.; Lang, O.; Pettenkofer, C.; Jaegermann, W.; Nebesny, K. W.; Lee, P. A.; Parkinson, B. A.; Armstrong, N. R. *J. Vac. Sci. Technol., A* **1995**, *13*, 1761.
(35) Njoroge, W.; Wöltgens, H.-W.; Wuttig, M. *J. Vac. Sci. Technol., A* **2002**, *20*, 230.
(36) Gladfelter, W. L. *Chem. Mater.* **1993**, *5*, 1372.